

2012

# The Effects of Fatty Desposits on the Accuracy of the Fibroscan Liver Transient Elastography Ultrasound System

S. Cournane
*Trinity College Dublin*

Jacinta Browne
*Technological University Dublin*, jacinta.browne@tudublin.ie

Andrew Fagan
*St. James's Hospital*



## Recommended Citation

Cournane, S., Browne, J.E., Fagan, A. J.:The Effects of Fatty Desposits on the Accuracy of the Fibroscan Liver Transient Elastography Ultrasound System. Physics in Medicine and Biology, Vol.57, no. 12, 2012, pp. 3901-3914. doi:10.1088/0031-9155/57/12/3901

# The effects of fatty deposits on the accuracy of the Fibroscan® liver transient elastography ultrasound system

**S Cournane[1], J E Browne[2] and A J Fagan[1,3]**

[1]Dept. Medical Physics & Bioengineering, St. James's Hospital, Dublin 8, Ireland
[2]Medical Ultrasound Physics and Technology Group, School of Physics & FOCAS Institute, Dublin Institute of Technology, Kevin's Street, Dublin 8, Ireland.
[3]Centre for Advanced Medical Imaging, St. James's Hospital / Trinity College Dublin, Ireland

**Abstract**

A new generation of ultrasound transient elastography (TE) systems have emerged which exploit the well-known correlation between the liver's pathological and mechanical properties through measurements of the Young's elastic modulus; however, little work has been carried out to examine the effect that fatty deposits may have on the TE measurement accuracy. An investigation was carried out on the effects on the measurement accuracy of a transient elastography ultrasound system, the Fibroscan®, caused by overlaying fat layers of varying thickness on healthy liver-mimicking phantoms, simulating in vivo conditions for obese patients. Furthermore, a steatosis effect similar to that in non-alcoholic fatty liver disease (NAFLD) and alcoholic liver disease (ALD) was simulated to investigate its effect on the TE system. A range of novel elastography fat-mimicking materials were developed using 6-10wt% poly(vinyl alcohol) cryogel capable of achieving a range of acoustic velocities (1482-1530m/s) and attenuation coefficients (0.4-1dB/MHz/cm) for simulating different liver states. Laboratory-based acoustic velocities and attenuation coefficients were measured while the Young's modulus was established through a gold standard compression testing method. A significant variation of the Young's elastic modulus was measured in healthy phantoms with overlaying fat layers of thicknesses exceeding 45mm, impinging on the scanners region of interest, overestimating the compression tested values by up to 11kPa in some cases. Furthermore, Fibroscan® measurements of the steatosis phantoms showed a consistent overestimation (~54%), which strongly suggests that the speed of sound mismatch between

that of liver tissue and that assumed by the scanner is responsible for the high clinical cut-offs established in the case of ALD and NAFLD.

## 1. Introduction

Elastography techniques for both estimating and imaging the mechanical properties of soft tissues have been of great interest for more than two decades (Ophir *et al.*, 1991; Céspedes *et al.*, 1993). A number of ultrasound elastographic approaches have been developed, such as static elastography, acoustic radiation force imaging (ARFI), transient elastography methods and shear wave imaging. Static elastography compares ultrasonic signals pre and post manual compression, thus identifying areas of increased relative stiffness (Ophir *et al*., 1991), while acoustic radiation force strain imaging uses an acoustic radiation force to produce an effective compression of the tissue (Nightingale *et al*., 2001; Mauldin *et al*., 2008). Transient elastography uses a low-frequency pulsed excitation to generate shear waves in the tissue, typically liver tissue as depicted in Figure 1, with the velocity of the shear wave, established to be related to tissue stiffness, measured with an ultrasound pulse-echo technique and used to calculate the elasticity (Sandrin *et al*., 2003). Shear imaging utilizes ARFI to generate shear waves in the tissue with the resultant shear wave velocities used to derive an elasticity map of the tissue which can then be overlaid on conventional ultrasound images (Sarvazyan *et al*., 1998; Bavu *et al*., 2010; Fink & Tanter, 2010). In recent years there has been an increase in the introduction of ultrasound elastography technology into the hospital environment, with transient elastography (TE) having become one of the more established elastography techniques in the clinical setting (Sandrin *et al.*, 2003; Bavu *et al.*, 2010; Evans *et al.*, 2010). The current gold standard for classification of liver fibrosis is through biopsy and histopathological analysis (Zhou and Lu, 2009), an invasive process which categorises five fibrotic stages of the liver according to the METAVIR classification, ranging from F0, regarded as a healthy liver state, to F4, the most severe stage of fibrosis (Bendossa and Poynard, 1996). Several studies have compared the METAVIR classification with stiffness values reported by the Fibroscan® system showing excellent correlation between the two and, hence, cutoff values have been established for various liver diseases in order to differentiate between fibrotic stages (Castera *et al.*, 2008). For instance, a typical range of 2.7 – 7 kPa has been established as a cutoff for the F0 – F1 stage in a viral hepatitis C study (Castera *et al.*, 2008), while 4.8 ± 0.9 kPa has been established as a healthy liver stiffness for a study on NAFLD (Yoneda *et al*., 2008). While non-invasive transient elastography is emerging as a credible alternative to the invasive biopsy procedure, the Fibroscan® has been reported to significantly overestimate the absolute shear elastic modulus values measured when compared with ‘gold standard’ mechanical testing (Cournane *et al.*, 2010). Furthermore, the system has been reported to rely on a single-point acoustic velocity calibration and on an

assumption that the liver is approximately elastic, when in fact liver tissue can have a wide range of acoustic velocities and is regarded as highly viscoelastic (Cournane *et al.*, 2010; Asbach *et al.*, 2008). Accordingly, although transient elastography techniques can provide clinically useful information, there remains a need to identify limitations of the technique to facilitate informed clinical interpretations of results.

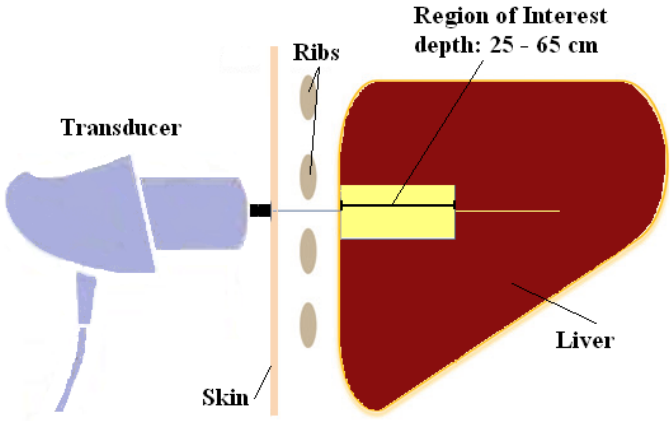


**Figure 1** Schematic of a transient elastography system used for measuring liver stiffness.

One concern with transient elastography is the effect that the presence of fatty deposits and fat tissue layers may have on the accuracy of the measured shear elastic modulus. Indeed, an identified shortcoming of the Fibroscan®, and its standard "M" probe, has been the unreliability in scanning patients of increased body mass index (BMI), where increased subcutaneous fat thickness has interfered with the intended interrogated region of the liver. This prompted the development of the "XL" probe which, in one study, was reported to successfully scan up to 59% of obese patients (BMI > 30kg/m$^2$) who could not be scanned using the M probe (de Lédinghen *et al.*, 2010). The XL probe is further reported to provide greater penetration depth due to its lower frequency ultrasonic signal while also sampling the elastogram from a deeper region, in order to avoid the fatty tissue layer. While the use of the XL probe leads to a higher success rate for valid measurements on obese patients, no study detailing the accuracy of the shear elastic modulus measurements has been carried out, and moreover, little is known about the effect that fatty deposits have on the Young's elastic modulus accuracy. Of the range of chronic liver conditions that can lead to fibrosis of the liver, non-alcoholic fatty liver disease (NAFLD), accounting for up to 60% of chronic liver cases in obese patients, encompasses a range of liver abnormalities characterised by macrovesicular hepatic steatosis (Miele and Forgione, 2007; Yoneda *et al.*, 2008), while alcoholic liver disease can also result in increased amounts of fatty deposits in the liver (Yang, 2008). The effect that this increased fat content, either overlaying the liver or in the organ itself, may have on transient elastography stiffness measurements has yet to be

assessed. Numerous clinical studies have been conducted to establish patient cut-off limits using the Fibroscan®; however, no physics studies have been conducted to investigate the affect of fat content on its accuracy.

Subcutaneous and intraperitoneal fat are generally considered a hindrance to good B-mode image resolution in conventional ultrasound imaging in clinical practice. The main cause of the degradation, taking the form of noise and clutter, is reported to stem from the composition of the body wall where fat, skin layer thickness and hydration level may all contribute in some way to the beam distortion and scattering (Browne *et al.*, 2005). While it has been somewhat established how the presence of fatty tissue may affect B-mode scanning, it is not known how fatty tissue may affect elastography imaging and quantitative stiffness measurement. Given that approximately 500 million people worldwide were regarded as clinically obese in 2008, with obesity levels ever-rising, having doubled since 1980 (WHO, 2011), combined with the ever-increasing use of elastographic techniques for diagnosis, there is a need to understand what effect the presence of fatty tissue may have on elastographic measurements.

The increased use of elastography techniques in the clinical setting has stimulated the development of tissue-mimicking material (TMM) phantoms for testing the capabilities of this relatively new technology (Cournane *et al.*, 2012). TMMs previously produced for use in elastography phantoms include oil-in-agar, oil-in-gelatin and agar dispersions (Madsen *et al.*, 2005), co-polymer in oil (Oudry *et al.*, 2009), polyacrylamide gels (Klinkosz *et al.*, 2008; Lou and Konofagou, 2009) and the poly(vinyl alcohol) cryogel (PVA-C) (Cournane *et al.*, 2010). In particular, PVA-C has been successfully used to assess the accuracy of transient elastography, with the properties of the material optimised to best represent the acoustic and shear elasticity properties of a range of liver tissues ranging from healthy to cirrhotic (Cournane *et al.*, 2010). There are no published studies describing fat-mimicking materials used for transient elastography; however, materials such as olive oil, lard and fish oil capsules have been used to mimic fat in studies assessing the effect of fat on conventional ultrasound B-mode imaging image quality performance. The use of olive oil, whose acoustic velocity of 1490 m/s and an attenuation coefficient of 0.87 dB/cm at 3MHz closely matches that of fat, has been used to introduce phase aberrations usually caused by subcutaneous fat layers, and was found to significantly reduce contrast resolution in B-mode scanning (Browne *et al.*, 2005). The inclusion of olive oil into agar based TMMs has also been successfully used to simulate subcutaneous fat in the breast in a study involving the development of clinically relevant quality assurance and anthropomorphic training phantoms (Cannon *et al.*, 2011). Furthermore, an elastography breast phantom was developed wherein the subcutaneous fat

was mimicked using an oil-in-gelatin dispersion in which it was possible to achieve different mechanical, acoustic and nuclear magnetic resonance properties by varying the volume percentages of oil (Madsen *et al.,* 2006); however, the elastic modulus values achieved were of the order of 20 kPa, much higher than the values required for mimicking liver tissue.

The aim of the current study was to investigate the effects that fatty deposits have on the measurement accuracy of a commercially available liver transient elastography system. It was of interest to consider two separate scenarios, one with a layer of fat overlying the liver, and a second with fatty deposits distributed uniformly throughout the liver, since both situations present clinically and yet both represent quite different technical challenges to the elastography system. To this end, a novel range of custom test phantoms were developed to mimic both overlying fat layers and fatty liver tissue. This is the first study of this type, firstly, to construct an elastography phantom specifically for mimicking fat and, secondly, to investigate the effects that fat content may have on elastography ultrasound results. Such a study was necessary and timely given the increasing levels of obesity on a global scale, coupled with the increased interest in ultrasound elastography for use in the clinical setting.

## 2. Materials and Methods

Given the ability to tailor the properties of PVA-C to mimic a wide range of acoustic properties relevant to both healthy and cirrhotic liver tissue, together with previous work using olive oil dispersions to mimic fat, these materials were chosen for use in the current study. Indeed, PVA-C has also been shown capable of achieving a range of stiffness values similar to those of the liver, thus presenting as an ideal TMM for this study. The preparation method of PVA-C phantoms for mimicking the acoustic and Young's elastic modulus properties of a range of healthy to cirrhotic liver tissue has previously been described in detail, and thus for a full description of this method the reader is referred to Cournane *et al.*, (2010). In the current study, the preparation of the fat PVA-C phantoms is described following a similar procedure to the liver PVA-C phantoms with the added measure of incorporating olive oil into the PVA mixture.

### *2.1 PVA-C phantom preparation*

99+% hydrolysed poly(vinyl alcohol) powder (Sigma-Aldrich® typical $M_w$ 89,000 – 98,000) was employed to produce 6, 8 and 10 wt% PVA solutions, respectively. 0.05 wt% concentration benzalkonium chloride was used as an antibacterial agent while 2 wt% of 0.3 $\mu$m aluminium oxide ($Al_2O_3$) (Logitech ultrafine Aluminium Oxide powder, LOT O81236) was included as acoustic scatterers. Separately, an olive oil component was made up using 90 wt% olive oil, 9 wt% degassed water and 1 wt% Synperonic A7 surfactant. This was

produced by initially mixing the surfactant and water together and heating to 50 ºC, to ensure a homogenous solution, before adding olive oil and blending with a domestic hand blender. Once blended, the olive oil component was added to the PVA mixture and stirred until a homogenous mixture containing 0 – 35 % by weight olive oil component was produced. This mixture was used to produce phantoms for fatty liver experiments and for fat layers overlaying a healthy liver phantom. In order to produce normal liver phantoms (Phantom numbered 1 – 4 with no overlaying fat layers), 13% by weight glycerol ($C_3H_8O_3$) was mixed with the initial PVA solution in preparation for processing. The mixtures, either for the fat experiments or the healthy liver experiments, were poured into airtight moulds, creating a humid environment to ensure no skin formed on the surface of the solution while cooling to room temperature, and left to rest for an additional 2 hours to allow for the removal of air bubbles. Solidification of the PVA samples was induced by a series of 24-hour freeze/thaw cycles (Cournane *et al.,* 2010). In cases where investigations of the physical and acoustic characteristics of the phantoms were carried out, the samples were sectioned after being allowed to condition, reaching thermal equilibrium with the ambient temperature, for 3 hours prior to sectioning (ISO-7748, 2008).

A number of experiments were carried out, wherein the phantoms' constituent ingredients were varied, to optimise the materials tissue-mimicking properties to best mimic a range of fatty, healthy and fibrotic liver tissue. To this end, 6, 8 and 10 wt% PVA solutions with 0 – 35% olive oil component, including $Al_2O_3$ acoustic scatterers and benzalkonium chloride were used to produce phantoms of diameter 6.7 cm and thickness 2.5 cm, processed through 2 freeze/thaw cycles. In addition, the effect of progressive 1 – 5 freeze/thaw cycling, respectively, on 5 fat phantoms was investigated using 6% PVA solution with a 35 wt% olive oil component and acoustic scatterers and anti-bacterial agent. To mimic fat layers, 6 wt% PVA solution with 35% by weight olive oil mixture including 2% by weight 0.3μm $Al_2O_3$ scatterers and the anti-bacterial agent were processed through 3 freeze/thaw cycles to create both fat layer phantoms (Fat layers ranging from 15 – 55 mm in depth) and fatty liver phantoms (Phantoms numbered 5 – 9). Furthermore, normal liver phantoms (Phantoms no. 1 – 4) were constructed using 6 wt% PVA solution, 13 wt% glycerol, 2% by weight 0.3μm $Al_2O_3$ scatterers and processed through 2 – 5 freeze/thaw cycles, respectively.

*2.2 Acoustic and Mechanical characterisation of the TMMs*

The TMM samples' acoustic velocity and attenuation coefficient were determined using an in-house built scanning acoustic macroscope (SAM) system (Cournane *et al.,* 2010), which utilises the pulse-echo substitution (Browne *et al.,* 2003). The SAM system consisted of a pulse receiver (Model 5052PR, Panametrics, UK), an immersion broadband transducer (5.15 -

9.44 MHz, Panametric, UK), a high-speed digitiser (250 MS/s, bandwidth of 125 MHz with 2 simultaneously sampled channels, National Instruments, USA), a water tank and a transducer holder. The transducer, submerged in a tank of degassed water (20 ± 0.5 °C), both transmitted and received ultrasonic pulses with the received RF signal, as reflected from the glass tank bottom, then amplified and outputted to the digitiser where it was saved for subsequent analysis. Scans were captured with and without TMM samples present in the path of the ultrasonic beam with the fast Fourier transform (FFT) spectra of both scans compared in order to determine the acoustic velocity ($c$) and the acoustic attenuation coefficient ($\alpha$) as a function of frequency. The acoustic velocity and attenuation coefficients of each sample, determined using 5 measurements on each sample, were calculated using the following equations:

$$\frac{1}{c_s} = \frac{1}{c_w} - \frac{\Delta t}{2d} \tag{1}$$

$$\alpha(f) = -\frac{20}{2d}\log_{10}\frac{A(f)}{A_0(f)} \tag{2}$$

where $d$, $\Delta t$, $c_s$ and $c_w$, are the thickness of the sample, the resultant time shift in the RF pulse with and without the sample in the path of the ultrasonic beam, and the acoustic velocities in the sample and degassed water, respectively. The attenuation as a function of frequency, $f$, was calculated from the log difference between the two spectra where $A$ and $A_0$ are the magnitudes of the signal with and without the sample in the path of the beam (Browne et al., 2003).

The phantoms were mechanically compression tested using a Lloyd Instruments LR30K*Plus* system (Ametek® measurement and calibration technology, USA) with a 500 N load cell. Samples were tested according to a standard compression protocol (ISO-7743, 2008) where metal plates were used to apply a compressive force to lubricated samples providing complete slip conditions such that the calculated modulus of the material was independent on the test piece shape. The compression stress was defined as the stress applied to cause a deformation of the test sample in the direction of the applied stress, expressed as the force divided by the original area of cross-section perpendicular to the direction of application of the force, or parallel to the compression plate face. The compression strain was defined as the deformation of the test piece in the direction of the applied stress divided by the original dimension in that direction and this is usually expressed as a percentage of the original dimension of the test sample. The compression modulus was the applied stress calculated on the original area of

cross-section divided by the resultant strain in the direction of application of the stress. Using this gold-standard technique, it is possible to provide measurements of the true mechanical properties of the phantoms (specifically, the Young's elastic modulus), against which the elastography system's measurements could be compared. Cylindrical samples, conditioned at the mechanical testing temperature (20 ± 0.5 °C) for the recommended 3 hours, were tested according to a standard compression protocol (ISO-7748, 2008). The machine operated at 50 mm/min until a strain of 30% was reached, with the strain then automatically released at the same rate, completing one compression and release cycle. Five cycles were completed with the mechanical properties of the phantom material calculated from the release stage data of the 5$^{th}$ compression and release cycle (ISO-7748, 2008). Samples were considered to be non-standard as defined by ISO 7743:2008, which states that for strains of up to about 30%, the relationship between stress and strain is given as:

$$\sigma = E\frac{\varepsilon}{1-\varepsilon} \tag{3}$$

where $\sigma$ , $\varepsilon$ and $E$ are the average stress, strain and Young's modulus, respectively. Indeed, in this study, the Young's elastic modulus values for each sample were determined for strains up to 10% where there was a linear relationship between stress and strain, given as:

$$\sigma = E\varepsilon \tag{4}$$

The uncertainties for the Young's modulus measurements were calculated by propagation of errors associated with the inherent precision limitations of the LR30K*Plus* system and the uncertainties of the linear least squares fitting (n = 5) of the stress-strain data.

*2.3 Transient elastography measurements*

The Fibroscan® (Echosens, France), composed of a shear elasticity probe and a dedicated electronic system and control unit, utilises a transient elastography technique to estimate the Young's elastic modulus of the liver. The original and possibly most commonly employed probe used with this system, the M probe, consists of a low-frequency piston-like vibrator with a single-element ultrasonic transducer operating at 3.5 MHz on the tip of the vibrator which operates in transmit/receive mode (Sandrin *et al.,* 2003). The shear wave, generated by the vibrator, is tracked using a cross-correlation technique which records the amplitude of the strain induced as a function of depth and time in the interrogated region. The elasticity of the region of interest (ROI) can be derived by calculating the velocity of the low frequency shear

wave located from 25 to 65 mm below the skin surface, as depicted in Figure 1. Thus, the Young's modulus is directly dependant on the shear velocity if dissipation in the medium is ignored (Sandrin *et al.,* 2003). The ROI in the case of the M probe has been set by the manufacturer for use on the general population to avoid the subcutaneous tissue and the liver fibrous capsule of the patient, and to ensure that the signal to noise ratio (SNR) of the ultrasound allows for good estimation of the tissue deformations. The ROI is thus not adjustable for different patients when using the M probe but it rather assumes that the liver is located in the region.

The setup used to measure the stiffness of the fatty liver phantoms via the Fibroscan® was similar to that already described in a previous study (Cournane *et al.,* 2010). The phantoms, typically with a diameter and height of 63 and 100 mm, respectively, were centred in a 92 mm diameter plastic container ensuring there was no contact with the container walls. A taut electrostatic discharge sheet (ESD) was used to overlay the top of the test objects in order to bear the majority of the force exerted by the Fibroscan® probe in order to reduce the potential for anisotropic effects. A thin film of water was present on top of the phantom to ensure adequate coupling. The probe was positioned orthogonally to the phantom, with 10 measurements recorded for each of the 5 fatty liver phantoms (Phantoms 5 – 9), respectively, returning the median stiffness value and interquartile range (IQR). In the case where fat layer phantoms (ranging from 15–55mm in depth) overlaying normal liver phantoms (Phantoms no. 1 – 4) were used to mimic subcutaneous fat overlaying a range of healthy to fibrotic liver tissue, the fat layer phantom was placed between the taut ESD sheet and the liver phantom, as depicted in Figure 2. 10 measurements were taken for each fat layer and liver phantom combination, with the median stiffness and IQR value recorded.

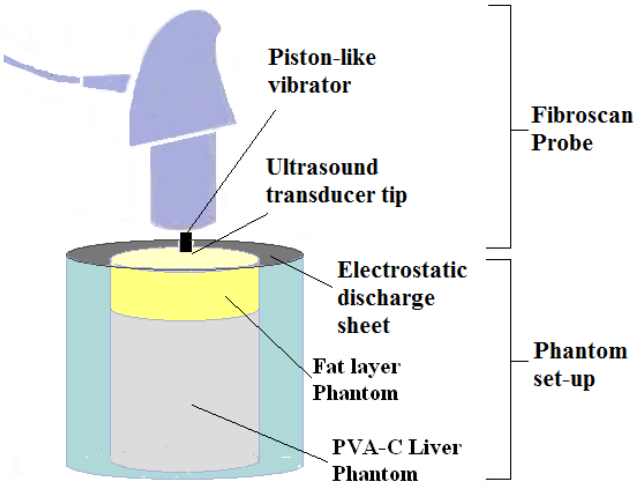


**Figure 2** Schematic of the experimental setup with fat layer phantoms overlaying healthy liver phantoms.

## 3. Results

*3.1 Acoustic velocity experiments*

The results of preliminary acoustic velocity experiments to empirically determine the suitable constituents for producing fat-mimicking phantoms are presented in Figure 3. Each data point represents the average of 5 measurements on each sample with the error bars representing the standard deviation (±σ). An increase in the olive oil content of the phantoms material produced test objects of relatively low acoustic velocity, while, in addition, a reduction in the PVA wt% solution resulted in a lower acoustic velocity. Accordingly, the TMM produced using 6% wt PVA solution with 35% olive oil solution exhibited suitable properties for fat layer and fatty liver phantoms.

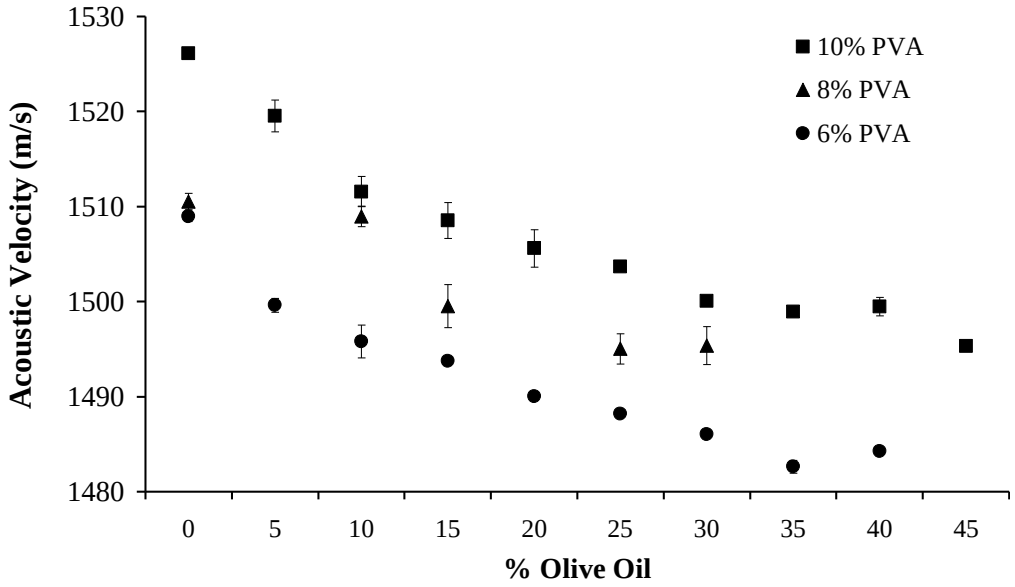


**Figure 3** The acoustic velocity (m/s) (±σ, n = 5 per sample) measured using the SAM system for a range of phantoms with 6, 8 and 10 wt% PVA and 0–35 wt% olive oil.

The effect of increased freeze/thaw cycling on the test object characteristics is shown in Figure 4(a), showing an increased shear elastic modulus, while, as evident from Figure 4(b) and 4(c), the acoustic velocity and acoustic attenuation coefficient are shown to be relatively constant.

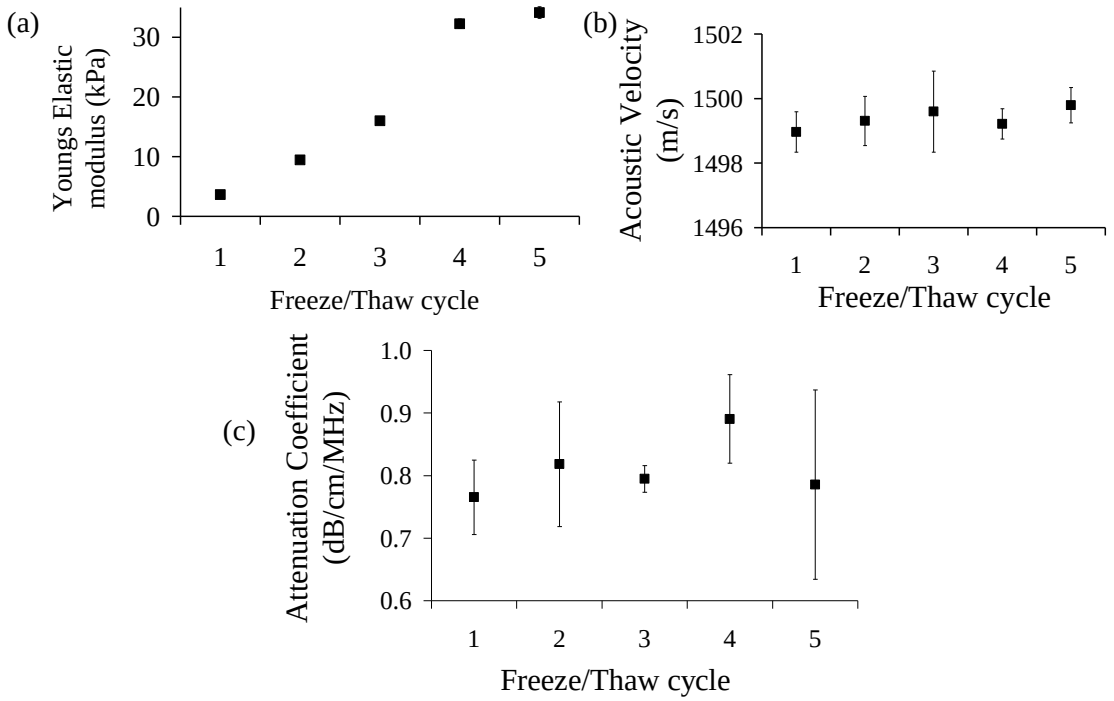


**Figure 4** (a) Young's elastic modulus (kPa) (±σ), (b) acoustic velocity (m/s) (±σ, n = 5 per sample) and (c) attenuation coefficient (dB/cm/MHz) (±σ, n = 5 per sample) with increasing f/t cycling.

*3.2 Overlaying Fat Layer experiments*

Figure 5 shows a comparison of the Young's elastic modulus values of a range of liver phantoms measured using the 'gold standard' compression testing technique and using the Fibroscan®, in addition to Fibroscan® measurements of the liver phantoms overlaid with fat layers of different thicknesses of 15, 25, 35, 45 and 55 mm. The compression tested shear elastic modulus values of the liver phantoms, produced by processing through $2-5$ freeze/thaw cycles, were between 4 to 8.1 kPa, an elastic modulus range representative of the early stages of fibrosis of the liver as established through empirical studies using the Fibroscan® system (Sandrin *et al.,* 2003; Caster *et al.,* 2008). The acoustic velocity of the liver phantoms was 1563 ± 4 m/s, which is within the typical range for healthy liver tissue (Lin *et al.,* 1987; Szabo, 2004) while the shear elastic modulus and acoustic velocity of the fat layers were 8.4 ± 1.6 kPa and 1491±2 m/s, respectively.

*3.3 Fatty Liver experiments*

A further investigation was carried out to observe the effect that fatty deposits in the liver, affecting a decreased acoustic velocity, may have on the measurement accuracy of the Fibroscan®. To this end, the Young's elastic modulus of 5 fatty liver phantoms, which had each been processed through 3 f/t cycles (Phantoms 5 – 9) , were measured using the

mechanical compression testing technique and the Fibroscan®; the results are presented in Table 1. The acoustic velocities and attenuation coefficients of the phantoms were measured to be 1500 ± 4 m/s and 0.8 ± 0.05 dB/cm/MHz, respectively.

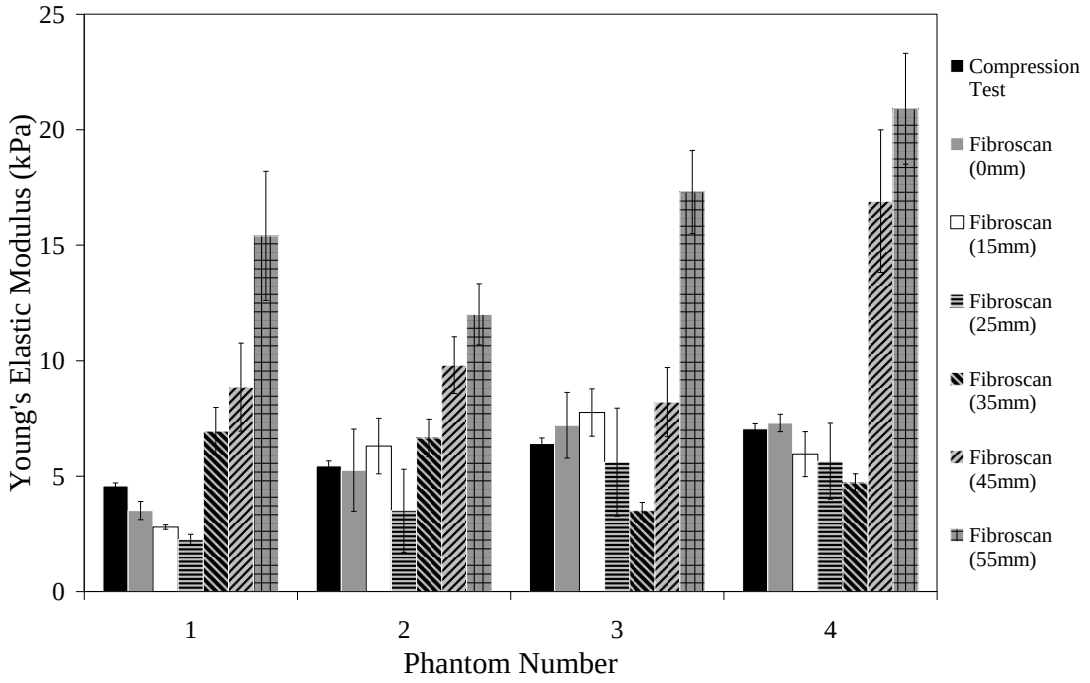


**Figure 5** Young's elastic modulus values of a range of liver phantoms (numbered 1 – 4) measured using the 'gold standard' technique (± σ) and compared with the transient elastography (± IQR/2) with a range of fat layers, of different thicknesses in the range 15 – 55 mm (as detailed in brackets in the legend), overlaying the liver phantoms.

**Table. 1** Young's elastic modulus values (kPa) of the fatty liver phantoms (5 – 9) as measured using the mechanical testing technique (±σ) and transient elastography (± IQR/2).

| Phantom Number | Mechanical testing | Fibroscan® |
|---|---|---|
| 5 | 16.0 ± 0.6 | 18.6 ± 0.7 |
| 6 | 11.2 ± 0.5 | 20.6 ± 0.9 |
| 7 | 13.5 ± 0.6 | 22.2 ± 1.4 |
| 8 | 9.7 ± 0.4 | 20.1 ± 0.8 |
| 9 | 13.8 ± 0.5 | 13.1 ± 0.7 |

## 4. Discussion

The Young's elastic modulus values achieved ranged from 3.6 – 34.1 kPa, encompassing the healthy to cirrhotic liver condition values observed in clinical studies using the Fibroscan®

(Sandrin *et al.*, 2003; Castera *et al.*, 2008). Accordingly, PVA-C with incorporated olive oil offered a novel means of assessing the accuracy of transient elastography when affected by fatty deposits. The acoustic velocity of fat in the body is documented to be in the range 1430 – 1500 m/s (Browne *et al.*, 2005; Szabo, 2004; Mast, 2000), while previous TMM studies mimicking the acoustic characteristics of fat have used TMMs with acoustic velocities of approximately 1490 m/s (Browne *et al.*, 2005; Madsen *et al.*, 2006). The optimum acoustic velocities produced in this study are thus in good agreement with values documented in the literature. The Young's elastic modulus of the fat layer is of the order of values previously reported for abdominal fat, measured *in vivo* to be 3.8 – 5.6 kPa (Nightingale *et al*., 2003),

Scanned measurements of the phantoms (Figure 5) show good correlation with the compression tested values; however, with the presence of the fat layers overlaying the liver phantoms, an increased uncertainty is evident. In the case of the 45 and 55 mm fat layers, a significant overestimation is apparent, with the scanned transient elastography Young's elastic modulus measurement overestimating the compression tested value by up to 11 kPa in some cases. This is most likely due to the impingement of the fat layers, measured to have a Young's elastic modulus of the order of the liver phantoms, on the ROI depth of 25 – 65 mm from where the stiffness measurement is calculated and due to the variation of the acoustic velocity in the ROI. It is assumed that the shear wave velocity is constant in the region of interest and, thus, the progression of the shear wave with depth will be linearly related to time. The Fibroscan® estimates the shear wave velocity by fitting a straight line to the slope of the strain induced as a function of depth and time. In the case where there are different layers with different Young's elastic modulus values or acoustic velocities, the relationship between the depth of the shear wave and time will thus be non-linear, resulting in an inaccurate calculation of the shear wave velocity. In Figure 6, elastograms are presented for the case of (a) no fat layer and (b) with a 45 mm thick fat layer, illustrating the modified appearance of the elastogram in the latter case, from which the Fibroscan® determines the shear wave velocity from a linear fit to the shear wave depicted (basically, from the slope of the line fitted to the data, illustrated as the white line in this figure). While the interference of the fat layers on the measurement ROI may contribute to the measurement discrepancy, the Young's elastic modulus values of the fat layers (8.4 ± 1.6 kPa) are much lower than those measured in the case of the 55 mm layer. This experiment simulates the case of an obese patient and highlights the increased unreliability when scanning patients with increased fat layers, concurring with clinical studies (de Lédinghen *et al.*, 2010). Furthermore, the overestimation encountered for thicker overlaying fat layers may have implications when considering the clinical management of obese patients. Phantoms 1 – 3 (Figure 5) should be categorised as healthy or mildly fibrotic (F0 – F1), according to the clinically established cut-

off values using the Fibroscan®; however, with a 55 mm overlaying fat layer, the Fibroscan® measurements indicates the liver to be in the latter fibrotic stages or cirrhotic stage (F3 – F4) when interpreted using these clinical cut-offs (Castera and Forns, 2008).

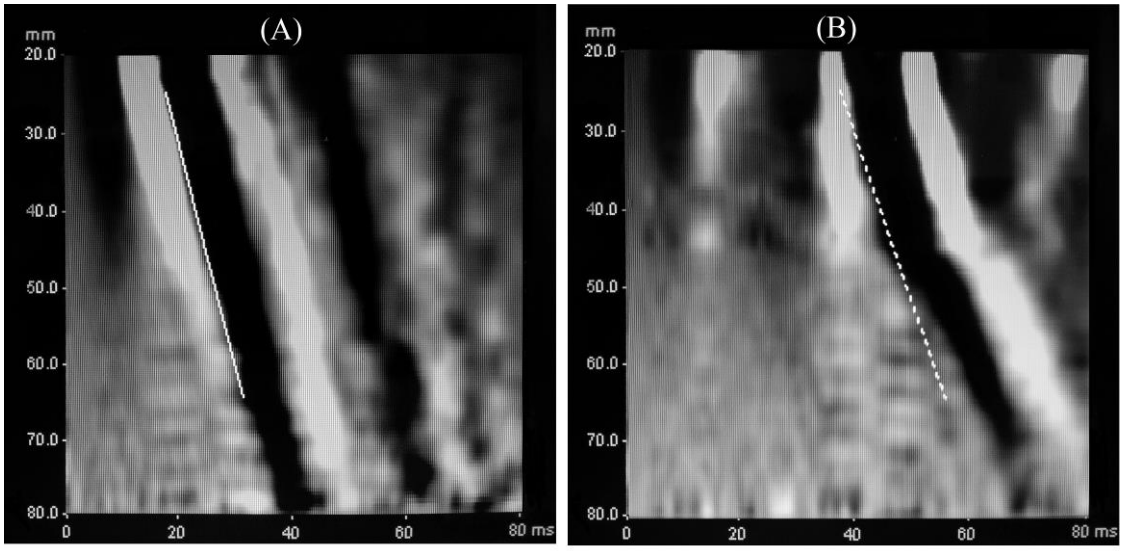


**Figure 6** Elastograms of a healthy liver phantom for the case of (A) no overlaying fat layer and (B) with a 45 mm thick overlaying fat layer, illustrating the modified appearance of the elastogram in the latter case. The Fibroscan® determines the shear wave velocity from a linear fit to the shear wave (white line), which is clearly problematic in the case depicted in (B).

Table 1 reveals a consistent overestimation of the shear elastic modulus for fatty liver measured using the transient elastography technique when compared with the 'gold standard' compression testing approach. Although there are variations in the Young's elastic modulus values of the produced fatty liver phantoms, due to variability in the production process, the relative difference between the gold standard and the Fibroscan® was of interest. Accordingly, a paired Student t-test indicated a significant difference between the data sets ($p < 0.013$), with an average percentage difference of the overestimation in the order of 54%. A likely cause of the observed discrepancy is the mismatch between the acoustic velocities of the constructed phantoms and that assumed by the Fibroscan®. In this case, since the acoustic velocity of the fat phantom is lower than that typically seen in the liver, the depth calculations will be inaccurate resulting in an overestimation of the shear wave depth and hence the shear wave velocity. Since the stiffness calculated by the Fibroscan® is related to the square of the shear wave velocity, the overestimation of the stiffness will be further increased. This acoustic mismatch has previously been suggested in the literature as a potential source of error given the single-point acoustic velocity calibration of the transient elastography system

and the range of acoustic velocity values observed in the liver for stages of fibrosis (Cournane *et al.*, 2010; Meziri *et al.*, 2005). Indeed, the overestimation of the absolute shear elastic modulus of the fat-mimicking phantoms offers an indication as to why the impinging fat layers in the previous investigation also caused an overestimation of the Fibroscan® measurements. A number of clinical studies have established cut-off stiffness values, measured using the Fibroscan® and correlated with biopsy results, in order to differentiate between the cirrhotic stage (F4) of the liver and the latter fibrotic stages (<F4). These cut-offs have been observed to be disease specific ranging from 17.5 kPa for NAFLD (Yoneda and Mawatari, 2008) to 22.6 kPa for alcoholic liver disease (ALD), while two different studies have determined cirrhosis cut-offs of 14.6 and 12.5 kPa for Hepatitis C (HCV) (Castéra *et al.*, 2005; Ziol *et al.*, 2005), and 10.6 kPa for Hepatitis B (HBV) (Marcellin *et al.*, 2005). In the context of this current study, the elevated established cut-off values determined for ALD and NAFLD, as compared with HCV and HBV, could be as a result of fatty deposits impinging on the measurement region of interest. Certainly, for both ALD and NAFLD the liver is known to exhibit increased fatty deposits when compared to conditions such as HCV and HBV (Yang, 2008), providing a likely reason for the differences in cut-off values.

Radiation force techniques, also capable of inducing shear waves *in vivo* in the human liver and estimating the Young's elastic modulus of liver tissue, can provide an alternative to transient elastography. The methods have established typical healthy liver elastic modulus values in the range 0.8 – 3 kPa and have also reported scanning to be unconstrained by obesity (Palmeri *et al.*, 2008) and to be capable of delivering acoustic radiation force to tissue depths of 8 cm (Fahey *et al.*, 2005). A more recent study has added that there is no correlation between BMI and stiffness when using ARFI and, indeed, in the case where the BMI > 40 $kg/m^2$, the increased BMI was not a limiting factor for ARFI (Palmeri *et al.*, 2011). Supersonic shear imaging (SSI) has also been identified as a means of assessing the health of the liver through stiffness measurement, establishing healthy liver tissue stiffness values to be of the order of 4.8 ± 0.8 kPa (Bavu *et al.*, 2010). When compared with the typical healthy liver stiffness value of 5 kPa established using the Fibroscan®, radiation force techniques indicate cutoff values to be much lower while SSI values are of the same order (Bavu *et al.*, 2010; Castera and Forns, 2008; Palmeri *et al.*, 2008). Accordingly, one recent study has recorded differences in stiffness measurements between ARFI and transient elastography, with ARFI proving more accurate than transient elastography for the non-invasive staging of both significant and severe classes of liver fibrosis (Rizzo *et al.*, 2011). This difference may be as a result of the elastography technique-specific generation of the shear waves in addition to the acoustic velocity values assumed by the different scanners for the interrogated tissue. Furthermore, while the liver is assumed to be elastic in the case of transient elastography, it is,

rather, viscoelastic (Asbach *et al.*, 2008) and thus the stiffness values measured with transient elastography techniques may not accurately reflect those mechanical properties measured by other methods. Indeed, if it is assumed that the liver is viscoelastic, it would be necessary to include a viscosity component in calculating the Young's modulus. Thus, clinical cutoffs established by the Fibroscan® should not be used for other emerging techniques until comprehensive clinical studies are conducted or unless empirical evidence suggests otherwise.

In conclusion, for transient elastography measurements of the Young's elastic modulus of liver phantoms, the presence of overlaying fat layers leads to an increased error of the stiffness values and also significant overestimation of the stiffness when using fat layers thicker than 45 mm. In addition, a further significant overestimation of the shear elastic modulus values was observed in steatosis liver phantoms compared to measurements made using a gold standard compression testing technique, most probably due to the mismatch between the acoustic velocities of the constructed phantoms and that assumed by the transient elastography scanner. This effect may be responsible for the high clinical liver stiffness cutoff values established for ALD and NAFLD, which may not reflect the absolute Young's elastic modulus values due to the presence of fatty deposits in the clinical populations examined. Similarly, in the case of obese patients, transient elastography measurements in the presence of overlaying fat layers could lead to patient mismanagement if the stiffness values are the sole means of diagnosis. As this new generation of ultrasound elastography systems become more prevalent in the clinical setting, it is imperative that clinicians relying heavily on such physics-based instrumentation for patient management are fully aware of the method's capabilities so that it may be used appropriately. The provision of comprehensive training for users is critical in this context.

**ACKNOWLEDGEMENTS**

The authors would like to acknowledge grant funding from the Research Support Unit in the Dublin Institute of Technology, and from the Health Research Board, Ireland.

**REFERENCES**

Asbach P, Klatt D, Hamhaber U, Braun J, Somasundaram R, Hamm B and Sack I 2008 Assessment of liver viscoelasticity using multifrequency MR elastography. *Magn Reson Med* **60** 373-9

Bavu E, Gennisson J-L, Mallet V, Osmanski B-F, Couade M, Bercoff FM, Fink M, Sogni P. Vallet-Pichard A, Nalpas B, Tanter M and Pol S 2010 Supersonic shear imaging is a new potent morphological non-invasive technique to assess liver fibrosis. Part 1:Technical feasability. *J Hepatology* **52** S59-S182

Bedossa P and Poynard T 1996 An algorithm for the grading of activity in chronic hepatitis C. The METAVIR Cooperative Study Group. *Hepatology* **24** 289-93

Browne JE, Ramnarine K, Watson AJ and Hoskins PR. 2003 Assessment of the acoustic properties of common tissue-mimicking test phantoms. *Ultrasound Med Biol* **29** 1053-60

Browne JE, Watson AJ, Hoskins PR and Elliott AT 2005 Investigation of the effect of subcutaneous fat on image quality performance of 2D conventional imaging and tissue harmonic imaging. *Ultrasound Med Biol* **31** 957-64

Cannon LM, Fagan AJ and Browne JE 2011 Novel tissue mimicking materials for high frequency breast ultrasound phantoms. *Ultrasound Med Biol* **37** 122-35.

Castera L and Forns X 2008 Non-invasive evaluation of liver fibrosis using transient elastography. *J Hepatol* **48** 835-47

Castéra L, Vergniol J, Foucher J, Le Bail B, Chanteloup E, Haaser M, Darriet M, Couzigou P and De Lédinghen V 2005 Prospective comparison of transient elastography, Fibrotest, APRI, and liver biopsy for the assessment of fibrosis in chronic hepatitis C. *Gastroenterology* **128** 343-50

Céspedes I, Ophir J, Ponnekanti H and Maklad N 1993 Elastography: elasticity imaging using ultrasound with application to muscle and breast in vivo. *Ultrason Imaging* **15** 73-88

Cournane S, Cannon L, Browne JE and Fagan AJ 2010 Assessment of the accuracy of an ultrasound elastography liver scanning system using a PVA-cryogel phantom with optimal acoustic and mechanical properties. *Phys Med Biol* **55** 5965-83

Cournane S, Fagan AJ and Browne JE Review of Ultrasound Elastography Quality Control and Training Test Phantoms. *Ultrasound* (In Press)

de Lédinghen V, Vergniol J, Foucher J, El-Hajbi F, Merrouche W, Rigalleau V 2010 Feasibility of liver transient elastography with FibroScan using a new probe for obese patients. *Liver Int* **30** 1043-8

Evans A, Whelehan P, Thomson K, McLean D, Brauer K, Purdie C, Jordan L, Baker L and Thompson A 2010 Quantitative shear wave ultrasound elastography: initial experience in solid breast masses. *Breast Cancer Res* **12** R104

Fahey BJ, Nightingale KR., Nelson RC, Palmeri ML and Trahey GE 2005 Acoustic radiation force impulse imaging of the abdomen: Demonstration of feasibility and utility. *Ultrasound Med Biol* **31** 1185-98

Fink M & Tanter M 2010 Multiwave imaging and super resolution. *Physics Today* **63** 28-33

ISO-7748 2008 *Rubber, vulcanized or thermoplastic–Determination of compression stress-strain properties.* Sweden

Klinkosz T, Lewa CJ and Paczkowski J 2008 Propagation velocity and attenuation of a shear wave pulse measured by ultrasound detection in agarose and polyacrylamide gels. *Ultrasound Med Biol* **34** 265-75

Lin T, Ophir J and Potter G 1987 Correlations of sound speed with tissue constituents in normal and diffuse liver disease. *Ultrason Imaging* **9** 29-40

Luo J and Konofagou E 2009 Effects of various parameters on lateral displacement estimation in ultrasound elastography. *Ultrasound Med Biol* **35** 1352-66

Madsen EL, Hobson MA, Frank GR, Shi H, Jiang J, Hall TJ, Varghese T, Doyley MM and Weaver JB 2006 Anthropomorphic breast phantoms for testing elastography systems. *Ultrasound Med Biol* **32** 857-74

Madsen EL, Hobson MA, Shi H, Varghese T and Frank GR 2005 Tissue-mimicking agar/gelatin materials for use in heterogeneous elastography phantoms. *Phys Med Biol* **50** 5597-618

Marcellin P, de Ledinghen V, Dhumeaux D, Poupon R, Ziol M, Bedossa P, and Beaugrand M 2005 Non-invasive assessment of liver fibrosis in chronic hepatitis B using FibroScan. *Hepatology* **42** 715A

Mast TD 2000 Empirical relationships between acoustic parameters in human soft tissues. *ARLO* **1** 37-42

Mauldin FW, Haider MA, Loboa EG, Behler RH, Euliss LE, Pfeiler TW and Gallippi CM 2008 Monitored steady-state excitation and recovery (MSSER) radiation force imaging using viscoelastic models. *IEEE Trans Ultrason Ferroelectr Freq Control* **55** 1597-1610

Meziri M, Pereira W, Abdelwahab A, Degott C and Laugier P 2005 In vitro chronic hepatic disease characterization with a multiparametric ultrasonic approach. *Ultrasonics* **43** 305-13

Miele L and Forgione A 2007 Noninvasive assessment of fibrosis in non-alcoholic fatty liver disease (NAFLD) and non-alcoholic steatohepatitis (NASH). *Transl Res* **149** 114-25

Nightingale KR, Palmeri ML, Nightingale RW, and Trahey GE 2001 On the feasibility of remote palpation using acoustic radiation force. *J. Acoust. Soc. Am.* **110** 625-34

Nightingale KR, McAleavey S and Trahey G 2003 Shear-wave generation using acoustic radiation force: In vivo and ex vivo results. *Ultrasound Med Biol*, **29** 1715-28

Ophir J, Céspedes I, Ponnekanti H, Yazdi Y and Li X 1991 Elastography: a quantitative method for imaging the elasticity of biological tissues. *Ultrason Imaging* **13** 111-34

Oudry J, Bastard C, Miette V, Willinger R and Sandrin L 2009 Copolymer-in-oil phantom materials for elastography. *Ultrasound Med Biol* **35** 1185-97

Palmeri ML, Wang MH, Dahl JJ, Frinkley KD and Nightingale KR 2008 Quantifying hepatic modulus in vivo using acoustic radiation force. *Ultrasound Med Biol* **34** 546-58

Palmeri ML, Wang MH, Rouze NC, Abdelmalek MF, Guy CD, Moser B, Diehl AM and Nightingale KR 2011 Noninvasive evaluation of hepatic fibrosis using acoustic radiation force-based shear stiffness in patients with nonalcoholic fatty liver disease. *J Hepatology* **55** 666-72

Rizzo L, Calvaruso V, Cacopardo B, Alessi N, Attanasio M, Petta S, Fatuzzo F, Montineri A, Mazzola A, L'abbate L, Nunnari G, Bronte L, Di Marco L, Craxì A and Cammà C 2011 Comparison of Transient Elastography and Acoustic Radiation Force Impulse for Non-Invasive Staging of Liver Fibrosis in Patients With Chronic Hepatitis C. *American J Gastroenterology (In press)*

Sandrin L, Fourquet B, Hasquenoph J, Yon S, Fournier C, Mal F, Christidis C, Ziol M, Poulet B, Kazemi F, Beaugrand M and Palau R 2003 Transient elastography: a new noninvasive method for assessment of hepatic fibrosis. *Ultrasound Med Biol* **29** 1705-13

Sarvazyan AP, Rudenko OV, Swanson SD, Fowlkes JB, and Emelianov SY 1998 Shear wave elasticity imaging: a new ultrasonic technology of medical diagnostics. *Ultrasound Med Biol* **24** 1419-1435.

Szabo T 2004 *Diagnostic Ultrasound Imaging—Inside out.* Boston, MA: Elsevier

WHO 2011 WHO Fact Sheet No.311

Yang SS 2008 Alcoholic Liver Disease: Clinical and Sonographic Features. *J Med Ultrasound* **16** 140-9

Yoneda M and Mawatari H 2008 Noninvasive assessment of liver fibrosis by measurement of stiffness in patients with nonalcoholic fatty liver disease (NAFLD). *Dig Liver Dis* **40** 371-8

Zhou K and Lu L 2009 Assessment of fibrosis in chronic liver diseases. *J Dig Dis* **10** 7-14

Ziol M, Handra-Luca A, Kettaneh A, Christidis C, Mal F, Kazemi F, de Lédinghen V, Marcellin P, Dhumeaux D, Trinchet J and Beaugrand M 2005 Noninvasive assessment of liver fibrosis by measurement of stiffness in patients with chronic hepatitis C. *Hepatology* **41** 48-54